Journal of Applied Polymer Science

Polypropylene/Polyethylene Blends as Models for High-Impact Propylene–Ethylene Copolymers, Part 1: Interaction Between Rheology and Morphology

Cornelia Kock,[1] Markus Gahleitner,[1] Alois Schausberger,[2] Elisabeth Ingolic[3]
[1]Innovation Headquarters, Borealis Polyolefine GmbH, 4021 Linz, Austria
[2]Institute of Polymer Science, Johannes Kepler University Linz, 4040 Linz, Austria
[3]Institute for Electron Microscopy, Graz University of Technology, 8010 Graz, Austria
Correspondence to: C. Kock (E-mail: cornelia.kock@borealisgroup.com)

ABSTRACT: In this work, composition effects on interfacial tension and morphology of binary polyolefin blends were studied using rheology and electron microscopy. The amount of dispersed phase (5–30 wt %) and its type [ethylene–octene copolymer, linear low-density polyethylene (LLDPE), and high-density polyethylene] was varied, and the influence of different matrix materials was also studied by using a polypropylene homopolymer and a ethylene–propylene (EP) random copolymer. The particle size distribution of the blends was determined using micrographs from transmission electron microscopy (TEM). A clear matrix effect on the flow behavior could be found from the viscosity curves of the blends. Analyzing the viscosity of the blends applying the logarithmic mixing rule indicated a partial miscibility of the EP random copolymer with low amounts of the LLDPE in the melt. Micrographs from TEM also showed a clear difference in morphology if the base polymer is changed, with PE lamellae growing out of the inclusions or being present directly embedded in the matrix. To verify these findings, the interfacial tension was determined. The applicability of Palierne's emulsion model was found to be limited for such complex systems, whereas Gramespacher–Meissner analysis led to interfacial tensions comparable with those already reported in the literature. The improved compatibility when changing the matrix polymer from the homopolymer to the random copolymer allows the development of multiphase materials with finer phase structure, which will also result in improved mechanical and optical performance. © 2012 Wiley Periodicals, Inc. J. Appl. Polym. Sci. 000: 000–000, 2012

KEYWORDS: polypropylene; polyethylene; morphology; rheology; blends

Received 21 September 2011; accepted 2 July 2012; published online
DOI: 10.1002/app.38289

INTRODUCTION

Since its invention in 1954, polypropylene (PP) has passed through a continuous development, enabling this material to be used for high-demanding technical purposes. The development of new processes (polymerization in reactor cascades) and the exploitation of single-site catalyst technology for PP polymerization have especially broadened the property profile.[1,2] Additionally, the possibility of adding various fillers and modifiers leads to a broad producible product range.

The modification of this polymer with elastomers is of high importance because of the brittle nature of PP below its glass transition temperature (at $\sim 0^{\circ}C$ for homopolymers). In this way, the toughness of the material can be enhanced while keeping reasonable stiffness and expanding the application temperature range. In earlier times, the modification was carried out by melt blending of PP with suitable elastomers such as styrene/butadiene block copolymers or ethylene–propylene rubber (EPR) and ethylene-propylene-diene elastomer (EPDM).[3,4] In the last 20 years, the development of new polymerization hardware and catalysts allowed an *in situ* preparation of these materials in the polymerization reactors.[5] The key advantage of this production mode is the major saving of energy and cost because of elimination of an additional extrusion step.

In contrast to extruder blends where the type and amount of components can be controlled directly,[6–8] reactor-based systems[9–11] will derive their structure and performance from the interaction between catalyst, reaction conditions, and monomer feed. To understand the respective correlations and to be able to optimize the performance of materials, both the phase structure development and the effect of this phase structure on mechanical and optical properties need to be studied. In addition, a rather precise fractionation of the different components, such as crystalline PP matrix, amorphous EP elastomer, and crystalline

PE fraction, is required, for which temperature rising elution fractionation[12,13] and crystallization-induced fractionation[14,15] have been established in the polyolefin area.

The target of this study was twofold: On one hand, the interaction between component rheology and compatibility in defining the blend morphology should be studied. On the other hand, the resulting mechanical performance—as in turn defined by morphology and component mechanics—and the possibility to fractionate the blends into the original components should be checked. Some aspects of the latter part of the work have been published before.[13,15] The current work focuses on preparing and understanding a model series for later mechanical investigation and fractionation by combining a crystalline matrix with PE-based inclusions of different crystallinity. In practical systems, the role of these inclusions is to absorb the stress that occurs in the case of deformation. In this way, these factors prevent crack propagation and failure in the material. The impact properties of these materials are influenced by three different groups of parameters[9]:

- molecular weight, molecular weight distribution (MWD), and crystallinity of the matrix;
- particle size (distribution), volume fraction, and ethylene content of the rubber phase; and
- compatibility and adhesion of the phases.

Through the viscosity ratio and the compatibility in molten state, often expressed by the interfacial tension, the component selection will define the morphology (particle size distribution) together with the Capillary or Weber number of the mixing process, whereas other factors are intrinsic component properties. One way to determine the interfacial tension is directly from the rheological behavior, for example, the dynamic moduli of the blends and their components. For example, this can be done by curve fitting applying Palierne's emulsion model[16] or via relaxation time spectra applying the Gramespacher–Meissner analysis,[17] both of which have been tested in the current work. A key factor in these analyses is the knowledge of the particle size distribution from an independent analysis like image analysis on electron micrographs.[18,19]

EXPERIMENTAL

A model blend series based on two different base (matrix) polymers, a homopolymer and a homogeneous EP random copolymer and three different PE modifier types [high-density polyethylene (HDPE), linear low-density polyethylene (LLDPE), and an ethylene-*co*-octene (EOC) plastomer[20,21]] was investigated. The components were selected such that the viscosity ratio between matrix and disperse phase remained approximately constant; the key characteristics of the components are listed in Table I. All grades are commercial products supplied by Borealis AG, Austria (PP, HDPE and LLDPE) resp. by DOW Chemical, Midland, MI, USA (EOC). The PPs and the LLDPE are based on a Ziegler (Ti) catalyst, with the latter containing butene as comonomer. The HDPE is based on a Phillips (Cr) catalyst, whereas the EOC comes from a solution process with a single-site catalyst.

The three modifiers were added in an amount of 5–20 wt % to both base polymers at 20 wt % only for the EOC. All were compounded on a corotating twin-screw extruder (Thermo-Prism TSE24, Thermo Electron GmbH, Germany) of 24-mm screw diameter and a length to diameter ratio of 48 with a high-intensity mixing screw and a temperature profile at 180–220°C with a throughput of 10 kgh^{-1} and a screw speed of 50 rpm.

Table I. Properties of the Blend Components [Matrix Polymers (PP) and Modifiers (PE)]

	MFR (g/10 min)	M_w (kg mol^{-1})	M_w/M_n	ρ (kg m^{-3})	T_m (°C)
PP homopolymer	2.8	432	5.5	905	166
EP random copolymer	1.9	442	3.5	890	139
EOC	1.0	147	2.4	870	60
LLDPE	0.4	191	11.8	923	124
HDPE	1.2	153	11.1	958	132

MFR: melt flow rate (ISO 1133; 230°C for PP and 190°C for PE); M_w: weight-average molecular weight; M_w/M_n: polydispersity ratio with number-average molecular weight (both from high-temperature SEC); ρ: density at 23°C; T_m: melting temperature from DSC (ISO 11357).

For studying the phase morphology, the samples were investigated by transmission electron microscopy (TEM) on ultra-microtomed specimens after contrasting with ruthenium tetroxide to allow differentiation between regions of high and low crystallinity.[22] TEM images were recorded on a Tecnai G^2 12 from FEI Company (Hillsboro, OR, USA), equipped with a CCD camera (Gatan Bioscan, UK) at 100 kV acceleration voltage at the Center for Electron Microscopy Graz, Austria. To avoid any orientation of the particles, the samples from which the slices (of 85 nm thickness) were taken were prepared by melting them in vacuum at 200°C in a heated mechanical press.[18]

The particle size analyses were done using the software ImageJ.[23] The program works with binarized 8-bit images, which are created from the micrographs. The image analyzer will then count the number of particles found in a selected area and measure the area of each particle. If one assumes the particle to be perfectly spherical, the number– (r_n) and volume– (r_v) average particle radii can be calculated from the particle areas according to the following equations:

$$r_n = \frac{\sum_{i=1}^{N} n_i r_i}{\sum_{i=1}^{N} r_i}, \quad (1)$$

$$r_v = \frac{\sum_{i=1}^{N} n_i r_i^4}{\sum_{i=1}^{N} n_i r_i^3}, \quad (2)$$

where n_i is the number of particles in the radii range r.

The melting and crystallization behavior of the compositions were determined according to ISO 11357 with a TA-Instruments (Germany) 2920 Dual-Cell instrument. A heating and cooling rate of 10°C min^{-1} was applied in a heat/cool/heat cycle between 23 and 210°C. The crystallization temperature T_c was determined in the cooling step, and the melting temperature T_m in the second heating step. The results are summarized in Table II; here and in all further denominations, the following

Table II. Thermal Analysis Results (DSC) of All Investigated Compositions

Sample	T_m (°C)	ΔH_m (J g^{-1})	X_c (%)	T_c (°C)	ΔH_c (J g^{-1})	Polymer
PPEO20	165	84	50	117	81	PP
	60	2	n.c.	42	4	EOC
PPLD5	164	83	42	117	97	PP
	125	19	n.c.			LLDPE
PPLD10	164	86	46	117	106	PP
	124	13	n.c.			LLDPE
PPLD15	165	68	38	116	103	PP
	125	35	n.c.	111	0.7	LLDPE
PPLD20	164	79	47	115	103	PP
	124	37	n.c.			LLDPE
PPHD5	163	79	40	117	109	PP
	130	38	270[a]			HDPE
PPHD10	165	81	43	116	107	PP
	130	22	76			HDPE
PPHD15	163	79	44	117	110	PP
	130	41	95			HDPE
PPHD20	163	77	46	117	121	PP
	130	50	87			HDPE
RPEO20	139	63	38	97	56	R-PP
	64	5	n.c.	43	2	EOC
RPLD5	140	33	16	102	81	R-PP
	124	37	n.c.			LLDPE
RPLD10	141	32	17	103	71	R-PP
	125	43	n.c.			LLDPE
RPLD15	143	27	15	104	89	R-PP
	124	47	n.c.			LLDPE
RPLD20	141	31	18	104	91	R-PP
	123	57	n.c.			LLDPE
RPHD5	141	25	13	107	80	R-PP
	128	56	390[a]			HDPE
RPHD10	142	21	11	108	91	R-PP
	129	61	211[a]			HDPE
RPHD15	142	22	12	108	86	R-PP
	129	66	152[a]			HDPE
RPHD20	143	20	11	111	18	R-PP
	129	89	153[a]	109	84	HDPE

n.c., not calculated.
[a]Theoretical value.

abbreviations are used: PP for the PP homopolymer, RP for the EP random copolymer, HD for HDPE, LD for LLDPE, and EO for the EOC plastomer, followed by a number indicating the modifier content. For calculating the crystallinity of the PP and the HDPE fractions, the literature values of 209 J g^{-1} for PP and 289 J g^{-1} for HDPE were used.[24]

The MWDs of the samples were determined at 135°C with a GPC 220 chromatograph (Polymer Laboratories, Church Stretton, UK) equipped with a differential refractive index (DRI) detector (Polymer Laboratories) and a differential viscometer 210 R (Viscotek, Houston, TX). A set of two columns was used, packed with crosslinked styrene–divinyl benzene (PLgel® Mixed-A LS, particle size: 20 µm, length: 300 mm, inner diameter: 7.5 mm; Polymer Laboratories). 1,2,4-Trichlorobenzene (Acros Organics, Geel, Belgium) containing 0.0125 vol % of 2,6-di-*tert*-butyl-(4-methylphenol) was used as solvent and eluent after filtration through a 0.45-µm PTFE filter. Prior to entering the pump, it was degassed with an online degasser PL-DG2 (Erc, Kawaguchi City, Japan). The flow rate was set to 0.5 mLmin^{-1}. Polymer solutions with concentrations in the range of 2–3 mgmL^{-1} were prepared under purified nitrogen by shaking at 160°C for 2 h and filtrated through a 0.2-µm filter prior to injection.

All rheological measurements were done in dynamic mode according to ISO 6271-10:1999 on a Physica MCR 501 rheometer with a TC30 temperature controller and a CTD600 precision temperature chamber (Anton Paar, Graz, Austria). The geometry used was plate–plate with 25 mm diameter, and all analyses were performed at 200°C under nitrogen atmosphere to avoid thermal oxidation. Samples of adequate diameter were prepared by pressing the material at 200°C under vacuum for 30 min and analyzed by frequency sweeps at angular frequencies decreasing logarithmically from 628 to 0.001 rads^{-1}. The values of storage modulus (G'), loss modulus (G''), complex modulus (G^*), and complex viscosity (η^*) were obtained as a function of frequency (ω). The well-established Cox-Merz relation[25] was assumed to be correct. Assuming that the shear rate representative for the mixing process in the extruder is $\sim$ 100 s^{-1},[9] the viscosity ratio can be calculated from the measured dynamic viscosities of the respective components at an angular frequency of 112 rad s^{-1}. Whenever the zero-shear viscosity η_0 could not be determined directly in the investigated frequency range, it was calculated by applying the Carreau Yasuda model:[26]

$$\eta = \eta_0[1 + (\tau\dot{\gamma})^a]^{[(n-1)a]}. \quad (3)$$

In this equation, η_0 stands for the zero-shear viscosity, τ for the characteristic relaxation time, n is the power-law index, and the parameter "a" describes the broadness of the transition between Newtonian and power-law regions.

For the determination of relaxation time spectra from the measured dynamic moduli, the routine in Paar Physica Software Rheoplus32 (V2.66) was used. This software was also used for the calculation of the spectra and the dynamic moduli from the MWD. The parameters τ_e (entanglement relaxation time) and M_e (entanglement molecular weight) necessary for these calculations are polymer specific; however, these parameters depend on the amount of molecules having molar masses smaller than the critical molar mass M_c and the ratio of PP/PE in the case of copolymers. Therefore, the calculation of these parameters was not attempted *a priori*, but they were taken as a result of a proper comparison between measured moduli and moduli calculated from SEC-MWD. A Gaussian molar mass distribution was calculated using Wesslau's formula[27] [see eq. (4)]. The aim was to fit the measured moduli perfectly with those calculated

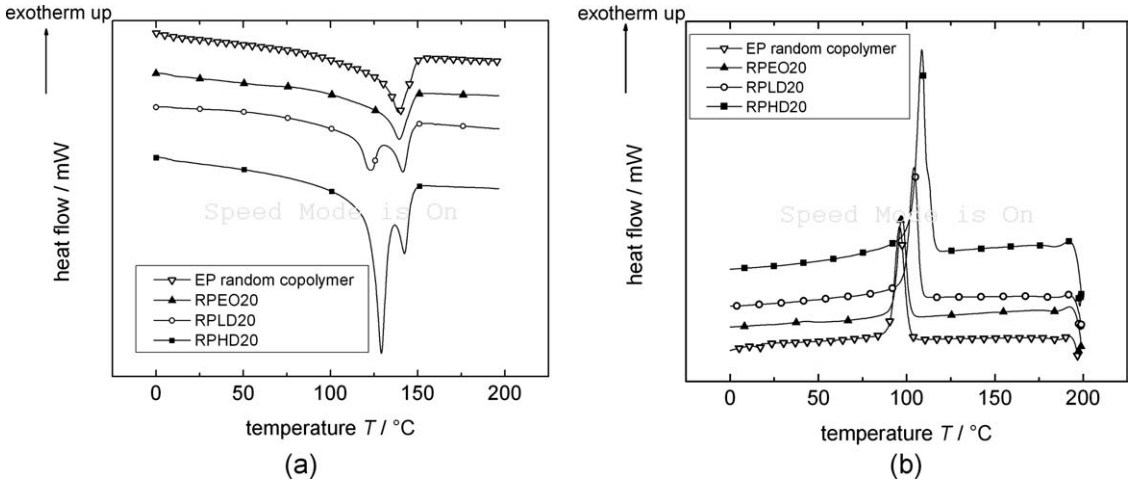

Figure 1. Melting and crystallization behavior of the model compounds with 20 wt % modifier based on the EP random copolymer: (a) melting endotherms and (b) crystallization exotherms (for the sake of clarity, the baselines of the curves are shifted along the *y*-axes).

from this distribution using predetermined parameters from the calculation of the moduli from the SEC-MWD.

$$w_i(M_i) = \frac{1}{\sqrt{2\pi}\sigma M_i} \exp\left\{-\frac{(\ln M_i/M_w)^2}{2\sigma^2}\right\}. \quad (4)$$

Here, w_i represents the weight fraction of a component i, M_i stands for the molar mass of the component i, M_w for the weight–average molar mass, and σ is a factor describing the broadness of the MWD.

RESULTS AND DISCUSSION

Thermal Analyses

In Figure 1, the DSC traces of the model compounds based on the EP random copolymer are shown as representatives of all model compounds. Although the melting endotherms show that the component peaks are separated, the crystallization peaks of the components are overlapping due to similar crystallization temperatures of base and modifier polymer.

It is possible to calculate the matrix crystallinity of the blends from the melt enthalpy of the base polymer assuming melt enthalpies for fully crystalline PP and HDPE as indicated above.[24] The results of these calculations show that the crystallinity of the model compounds is a function of the amount and the type of modifier polymer (see Table II). The influence of plastomer addition on the matrix crystallinity is negligible; however, an apparent decrease of matrix crystallinity is found for the PE modified samples. The fact that obviously meaningless values above 100% crystallinity are calculated for HDPE in some cases results from the difficulty to clearly separate the melting peaks (see Figure 1). This of course also limits the value of the respective PP crystallinities; however, conclusions on cocrystallization or even miscibility cannot be drawn from these data alone.

Blend Morphology

As the image analysis for determining the average particle sizes was very laborious, only the blends with 20 wt % of modifier were used for this determination. Figures 2 and 3 present the respective TEM images for these six compositions at the level of magnification used for determining the particle size distribution; distinct particle/matrix structures with little anisotropy are found at this length scale. No clear order of particle size can be

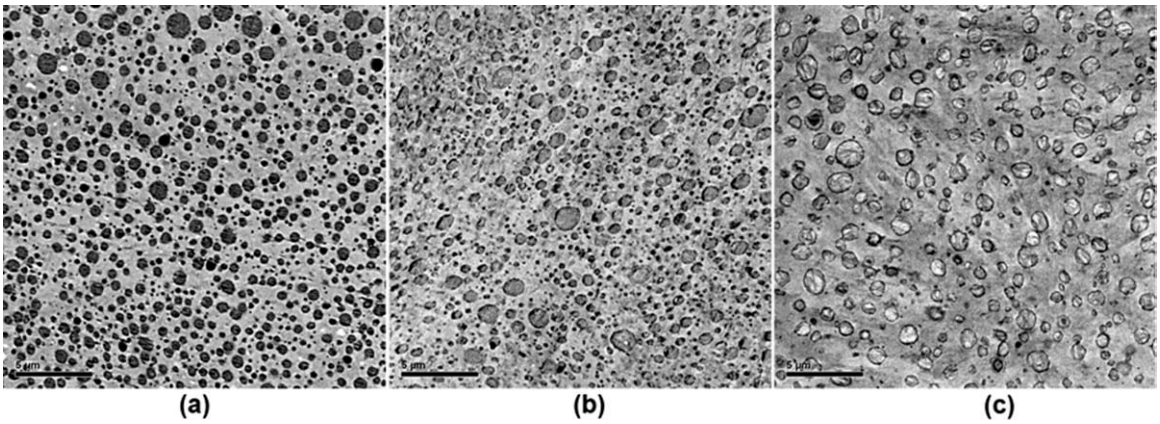

Figure 2. TEM images of 20 wt % blend series based on PP homopolymer: (a) PPEO20; (b) PPLD20; and (c) PPHD20.

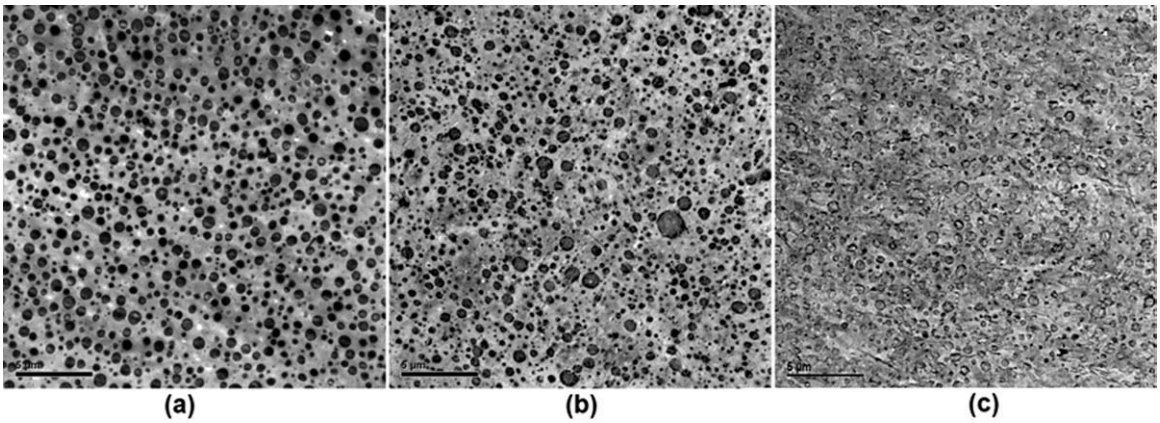

Figure 3. TEM images of 20 wt % blend series based on EP random copolymer: (a) RPEO20; (b) RPLD20; and (c) RPHD20.

directly identified from the images; however, the particles are generally smaller in the blends based on the EP random copolymer.

When checking the morphology of the blends at higher magnification, further details can be found. Both LLDPE and HDPE form distinct crystalline lamellae within the particles, in contrast to the EOC plastomer which is generally known to crystallize in a fringed micellae structure.[28] For RPHD20, PE lamellae are observable directly embedded in the PP matrix (see Figure 4). This finding can be interpreted as a partial miscibility of the two components, the isolated lamellae resulting from the crystallization of the material starting before the phase separation. Furthermore, clear indications exist in the literature for cocrystallization between PP and PE occurring under certain conditions.[29] This might result from the fact that the random copolymer contains some ethylene units or even polyethylene blocks along the chain, and thus, the compatibility with the modifier polymer (HDPE) is enhanced. For the LLDPE modified blends, the compatibility of the modifier with the matrix also appears to be enhanced for the EP random copolymer matrix. A clear difference in the interface between matrix and particles is seen when comparing the two matrix materials (see Figure 5). For the blend based on PP homopolymer, a smooth surface between inclusion and matrix is formed, and the PE lamellae are situated totally inside these inclusions. In contrast, the blends based on the random copolymer show LLDPE lamellae growing from the inside of the inclusion into the matrix. It can be concluded that EP random copolymers are more suitable as matrix for model compounds of heterophasic PP as the formed interface between particle and modifier is more similar to the ragged surface that can be found in reactor products.[30,31] Furthermore, the particle size distribution is broadest for the blends modified with LLDPE, irrespective of the base polymers used.

The modifier particles were measured and counted with the aid of the ImageJ analyzer to gain information concerning the average particle sizes. The number– and volume–average radii as well as the ratio of these two values to describe the broadness of the distribution are listed in Table III. For the volume fraction calculation, the weight fractions (w) were corrected with the component densities of Table I according to the following equation:

$$\Phi = \rho_M w_R / (\rho_M w_R + \rho_R w_M), \quad (5)$$

where ρ stands for the density of the materials, and the index M is indicating the matrix material and R the modifier polymer.

As already assumed from the visual interpretation of the images, the particle size distribution increases if the LLDPE is used as modifier polymer instead of the plastomer, and the values for r_n decrease with a change of the modifier from plastomer to LLDPE, irrespective of the base polymer used. This indicates a better compatibility of the polyethylene when compared with the plastomer with the base polymers used. The HDPE forms rather big inclusions in the PP homopolymer matrix; however, they are smaller in the EP random copolymer matrix. To clarify these assumptions, the viscosity ratios of the blends as well as their interfacial tension were determined by two rheological approaches, as outlined in detail below.

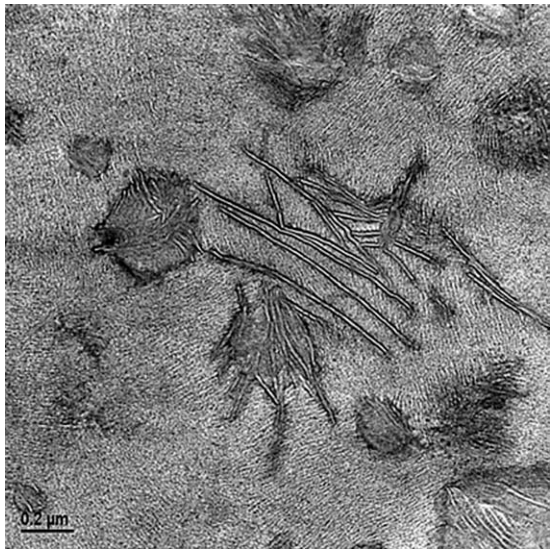

Figure 4. TEM image of ethylene–propylene random copolymer blended with HDPE (RPHD20) at higher magnification. PE lamellae are directly embedded in the PP matrix (scale bar: 0.2 µm).

Applied Polymer SCIENCE

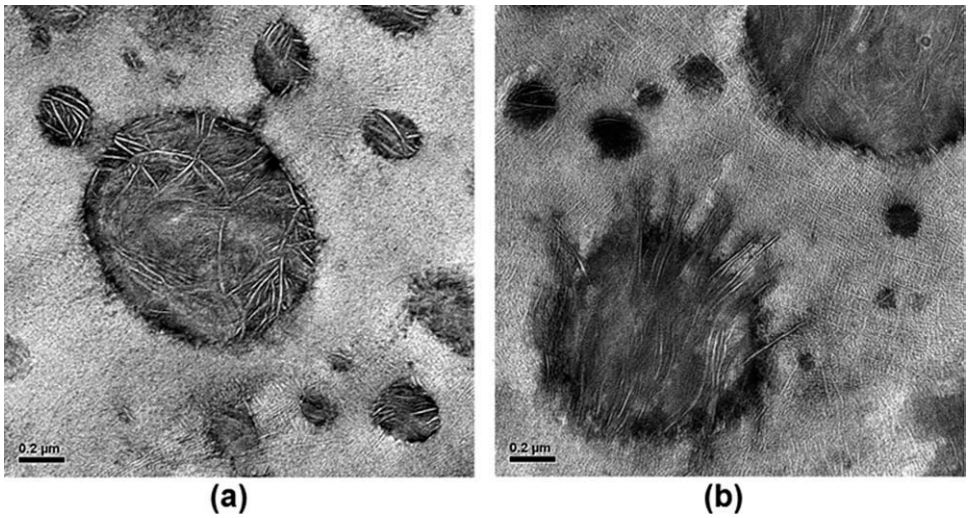

Figure 5. TEM images of blends modified with 20% LLDPE and different base polymers. Base material: (a) PP homopolymer, PPLD20 and (b) EP random copolymer, RPLD20 (scale bar: 0.2 µm).

Flow Curves of the Materials

The complex viscosities of the base and the modifier polymers are shown in Figure 6. As the base polymers all have comparable molecular weights, their viscosities do not differ strongly. Both base polymers also reach the Newtonian viscosity plateau, which is not the case for the HDPE. The reason for the strong increase in the viscosity of HDPE is that this polymer has a very broad MWD resulting from the polymerization process with a chromium catalyst. Furthermore, long-chain branches may be formed during polymerization by the copolymerization of vinyl end groups formed in chain termination by chromium catalysts.[32] The EOC plastomer shows the lowest viscosity, and because of its narrow MWD, the Newtonian viscosity plateau already starts at relatively high frequencies.

The same approach was used for the blends based on PP and EP random copolymer with different amounts of LLDPE. Additionally, η_0 of the blends was calculated from the zero-shear viscosities of the components through addition via the logarithmic mixing rule. As shown in Figure 7, the results fit very well until a modifier content of 15 wt % for LLDPE modified blends based on the EP random copolymer. At higher concentrations, deviations occur as increases in the measured zero-shear viscosities. This actually confirms that in the melt state, small amounts of LLDPE are miscible in the EP random copolymer. These results correspond with findings from the literature where miscibility of LLDPE and PP was investigated by means of DSC.[33–35] If, however, the EP random copolymer forms the matrix instead of the homopolymer, the deviations start at higher PE concentrations, indicating better miscibility of the components in the blend. Especially, the LLDPE shows a high degree of compatibility with respect to miscibility with the EP random copolymer in the melt up to 15 wt % modifier content.

Table III. Results of the Particle Size Analyses

Sample	r_n (µm)	r_v (µm)	r_v/r_n	Φ (vol %)
PPEO20	0.23	0.43	1.9	20.6
PPLD20	0.19	0.45	2.3	19.7
PPHD20	0.34	0.64	1.9	19.1
RPEO20	0.25	0.43	1.7	20.4
RPLD20	0.18	0.36	2.0	19.4
RPHD20	0.22	0.41	1.9	18.8

r_n: number-average particle radius; r_v: volume-average particle radius; r_v/r_n: parameter of the broadness of the particle size distribution; Φ: volume fraction of the dispersed phase calculated according to eqs. (1) and (2).

Relaxation Time Spectra

The entire behavior of a polymer is often described using the relaxation time spectrum as it only depends on material properties and not on experimental setups. It reflects the molecular processes taking place in a certain time frame. The transformation of experimentally obtained datasets of G', G'', and ω into relaxation time spectra is based on the following equations and

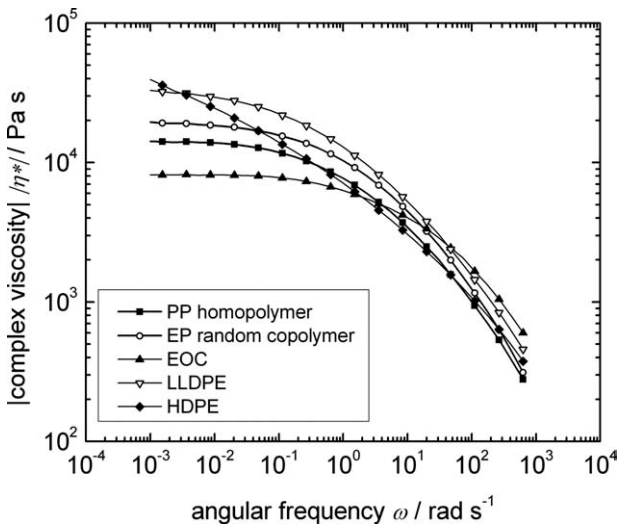

Figure 6. Complex dynamic viscosity (200°C) of the base and modifier polymers.

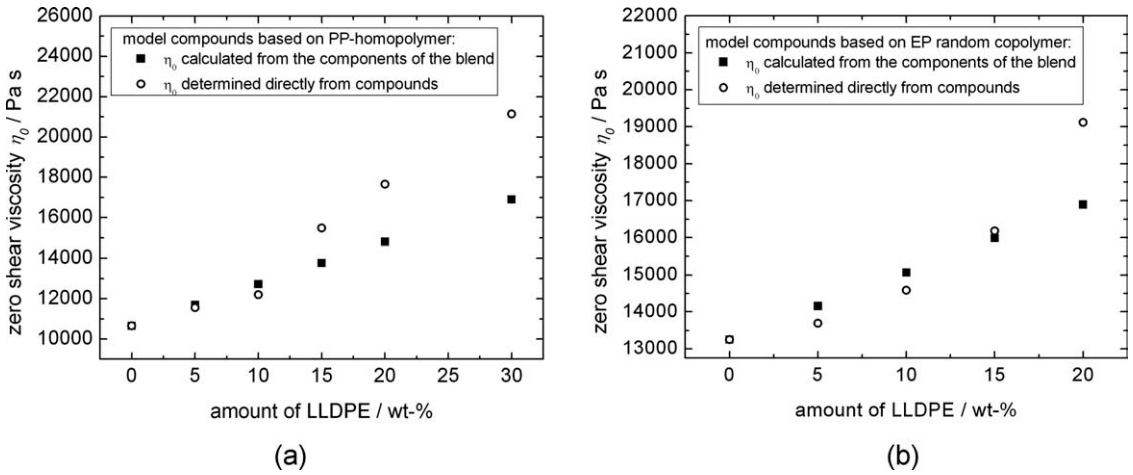

Figure 7. Comparison of the zero-shear viscosities of the blends calculated from zero-shear viscosities of the components and determined via flow modeling of the viscosity curves of the blends: (a) blends of PP homopolymer and LLDPE and (b) blends of EP random copolymer and LLDPE.

done by a regularization process.[36,37] A direct transformation is impossible because of a mathematically ill-posed problem.

$$G'(\omega) = \sum_{i=1}^{N} \frac{G_i(\omega\tau_i)^2}{[1 + (\omega\tau_i)^2]}, \tag{6}$$

and

$$G''(\omega) = \sum_{i=1}^{N} \frac{G_i(\omega\tau_i)}{[1 + (\omega\tau_i)^2]}. \tag{7}$$

Another approach to obtain the relaxation time spectra is its calculation from the MWD of the polymer. These calculations can be done applying the mixing rule of Schausberger and the Baumgärtel-Schausberger-Winter (BSW) spectrum.[38,39] This spectrum defines the relaxation modes of linear chains of equal length. Each component of molecules with a molar mass M_i is represented by its own spectrum. The leading relaxation time $\tau_{i,0}$ is directly connected to the molar mass M_i of the chain according to the following equations:

$$\tau_{i,0} = k \cdot M_i^{3.4}, \tag{8}$$

or

$$\tau_{i,0} = \tau_e \cdot \left(\frac{M_i}{M_e}\right)^{3.4}. \tag{9}$$

The leading relaxation strength $g_{i,0}$ of the leading relaxation time $\tau_{i,0}$ is proportional to the weight fraction w_i of the component M_i. In a polydisperse system, both $\tau_{i,0}$ and w_i are functions of the molar mass distribution, which is accounted for by a mixing rule. The sum of all relaxation strengths is the plateau modulus G_{N0}, which itself is related to the entanglement molar mass M_e according to the following equation:

$$M_e = \frac{\rho RT}{G_{N0}}. \tag{10}$$

In this equation, ρ is the density of the polymer, R is the ideal gas constant, and T is the temperature.

The only two polymer-specific parameters are the entanglement relaxation time τ_e and the entanglement molecular weight M_e. This method allows the determination of MWD of a polymer from rheology without any significant problems. This can be an advantage especially in the high molar mass region where SEC is not sensitive.

The relaxation time spectra of the base polymers and the modifiers were determined from measured SEC-MWDs and from calculated Gaussian MWDs. For the model compounds, the spectra were calculated from the dynamic moduli and from the Gaussian MWDs determined through a weighted addition of the distribution of the components. This allows the calculation of relaxation time spectra including and excluding the interfacial contribution, which is essential for Gramespacher–Meissner analysis.

For the base polymers, the SEC-MWD shows a negative deviation in the high molar mass region compared to the distribution calculated using Wesslau's formula (see Figure 8). Starting from a Gaussian distribution with a larger amount of long molecules one arrives at a perfect fit for measured and calculated moduli. Consequently, the relaxation time spectra determined from the Gaussian distribution also showed slightly higher relaxation strengths at longer times.

For the modifier polymers, the similarity of calculated and measured moduli was not as good as for the base polymers because of the more complex structure of the modifier polymers (side-chain branches). The average molecular weight derived from the Gaussian distribution is comparable with that obtained from SEC (see Table IV). The HDPE was not analyzed by this method as this will not lead to satisfying results because of the complex structure of the polymers. The Gaussian MWDs of the model compounds were calculated by a weighted summation of the Gaussian distributions of their components. Relaxation time spectra calculated from these will not reflect the part originating from the interfacial tension of the multicomponent systems. Thus, a total correlation between calculated and measured

Applied Polymer SCIENCE

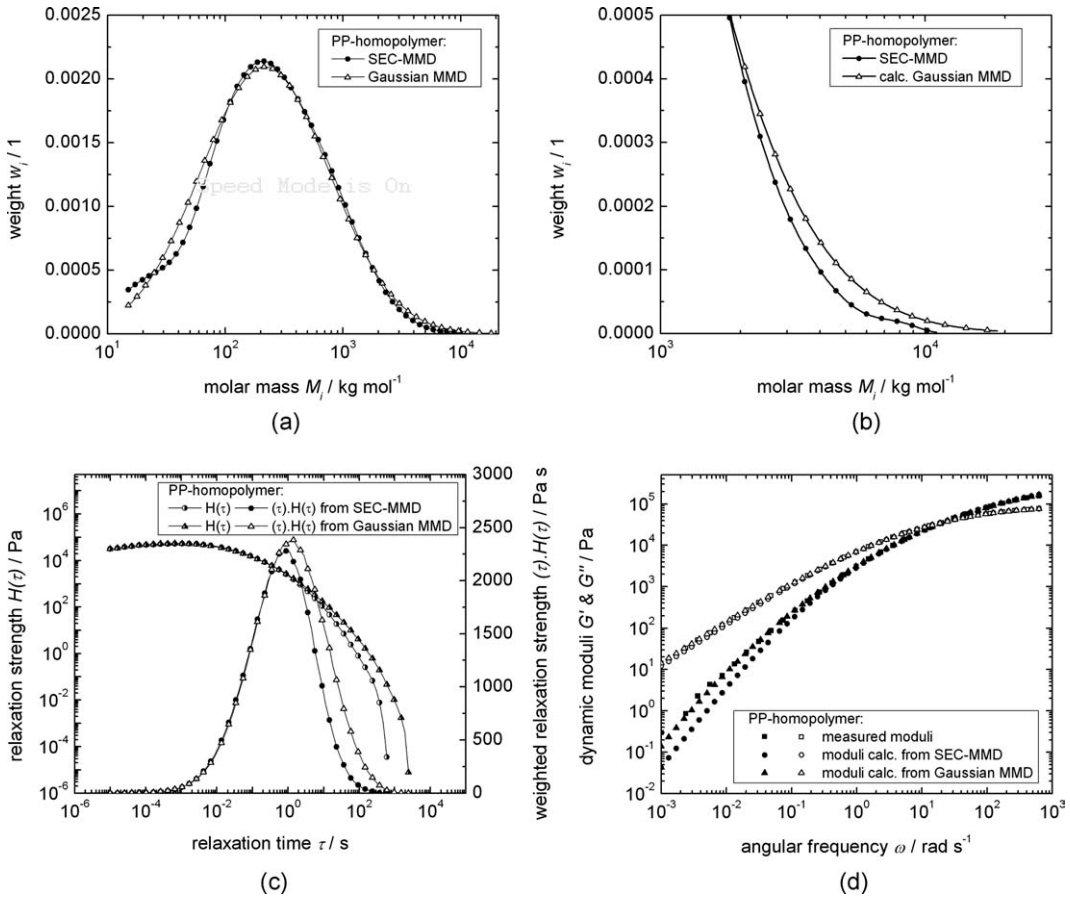

Figure 8. MWD, dynamic moduli, and relaxation time spectra of PP: (a) SEC-MWD compared with the Gaussian MWD; (b) enlargement of high molecular part of the MWDs; (c) from the MWDs calculated spectra; and (d) dynamic moduli measured and calculated from the two spectra.

moduli is not possible if one considers that the moduli calculated from the MWD will never show the increase of the storage moduli at low frequencies.

If the spectrum of the model compounds is calculated directly from the measured dynamic moduli, the effect of the interfacial tension is included. The part caused by the interfacial tension can be obtained if the spectrum calculated from the MWD is subtracted from the spectrum calculated from the moduli. The influence of the interfacial tension is very pronounced for incompatible blends, and a discrete second peak in the weighted relaxation time spectrum will be present (see Figure 9). The so-called droplet shape relaxation time τ_1 of the inclusions describes the relaxation of the inclusion droplet as a response to the applied stress. It was determined for all model compounds except those containing HDPE from the weighted relaxation time spectra. The observed values are listed in Table V; the high-shape relaxation times indicate good compatibility of the components. These results confirm the better compatibility of the matrix materials with the LLDPE than that with the EOC already assumed from the TEM morphology images.

However, to get more defined information on the compatibility of the components, the interfacial tension was calculated according to the theories of Palierne[16,40] and Gramespacher–Meissner.[17]

Palierne Analysis

The Palierne's emulsion model allows the calculation of the interfacial tension α from the dynamic moduli of the components and the resulting blend, provided that the volume fraction of the dispersed phase Φ and the particle size of the inclusions are known. The interfacial tension can be calculated according to eqs. (11) and (12).[40] As the particle size, the fraction of the dispersed phase, and the radii are known, the equations can be used in connection with the measured moduli of the components and the blend to estimate the interfacial tension. This is done through approximation of (α/r) until the best fit between experimental and calculated curves is obtained.

$$G_B^* = \frac{1 + 3\Phi B^*(\omega)}{1 - 2\Phi B^*(\omega)} \times G_M^*, \tag{11}$$

$$B^*(\omega) = \frac{\left[G_I^*(\omega) - G_M^*(\omega)\right] \times \left[16G_M^*(\omega) + 19G_I^*(\omega)\right] + 4\left(\frac{\alpha}{r}\right) \times \left[2G_M^*(\omega) + 5G_I^*(\omega)\right]}{\left[2G_I^*(\omega) + 3G_M^*(\omega)\right] \times \left[16G_M^*(\omega) + 19G_I^*(\omega)\right] + 40\left(\frac{\alpha}{r}\right) \times \left[G_M^*(\omega) + G_I^*(\omega)\right]}, \tag{12}$$

Table IV. Average Molecular Weights and Polydispersity of the Model Compounds

	SEC-MWDs			Gaussian distribution		
Sample code	M_n (kg mol^{-1})	M_w (kg mol^{-1})	M_w/M_n	M_n (kg mol^{-1})	M_w (kg mol^{-1})	M_w/M_n
PP	79	432	5.5	98	480	4.9
RP	127	474	3.7	120	505	4.2
PPEO20	78	445	5.7	85	420	4.9
PPLD20	56	412	7.4	53	425	8.0
PPHD20	48	520	10.8	26	386	14.8
RPEO20	96	458	4.8	94	384	4.1
RPLD20	62	448	7.2	54	406	7.5
RPHD20	86	740	8.6	23	399	17.3

The MWDs were determined via SEC and calculated with the Wesslau formula. M_n: number-average molecular weight; M_w: weight-average molecular weight; M_w/M_n: polydispersity.

with G^* being the complex moduli, Φ the volume fraction of disperse phase, B^* the so-called blending factor, α the interfacial tension between matrix and inclusions, and r the average radius of these inclusions. The indices refer to the blend (B), matrix (M), and inclusions (I).

The approach has been widely used for immiscible blends; Souza and Demarquette[41] reported that the interfacial tension of PP/HDPE blends has been determined via the Palierne model or by Gramespacher and Meissner analysis as a function of the HDPE concentration. Vincze-Minya and Schausberger[42] investigated the influence of the phase morphology on the viscoelastic behavior of PP/EPR blends (PP/EPR blends) by applying the same models. In none of these cases, composition effects have been studied.

All measured G' curves of the blends show a significant increase over the pure base polymer curve at low frequencies, which is more pronounced for the blends based on the EP random copolymer. The facts that the volume fraction of the modifier polymer is almost constant and that the viscosity ratio differences are limited allow the conclusion that average particle size and interfacial tension are decisive for this development (see Table IV). Increased interfacial tension leads to a reduction in the width of the plateau as it is observed for blends based on PP homopolymer when compared with blends based on EP copolymer.

The best agreement between blend curves calculated from the Palierne model and the measured ones can be achieved for the systems based on the PP homopolymer (see Figure 10). For the random copolymer, the correlation was not as good. One reason for this fact might be that the Palierne's emulsion model only predicts the rheological behavior of incompatible polymer blends and does not take into account interactions between matrix and inclusions, which will lead to an additional mean stress due to the interconnectivity.[43] As it was seen in the TEM images

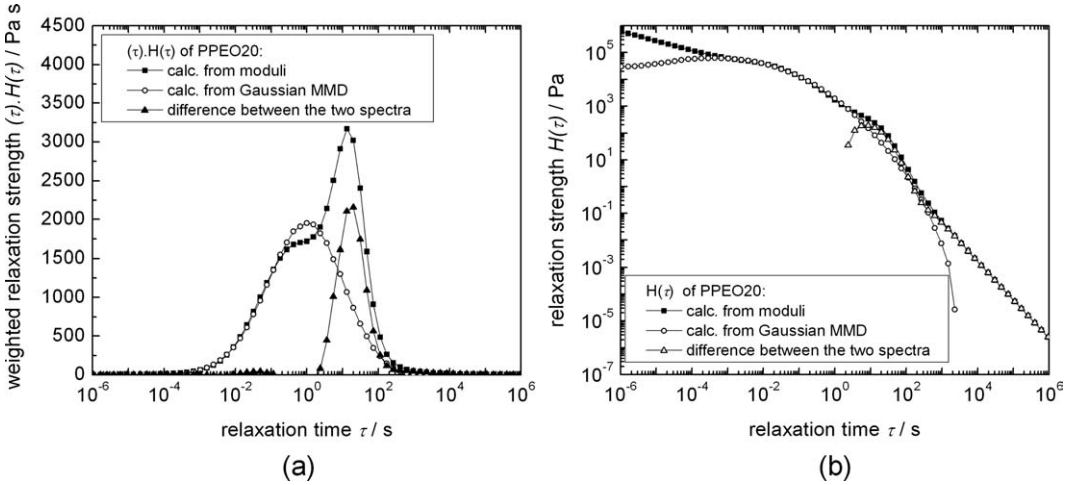

Figure 9. The influence of the interfacial tension on the relaxation time spectra of PPEO20: (a) weighted relaxation time spectra τ. $H(\tau)$ calculated from the dynamic moduli and from the MWD and the difference between them. (b) Comparison of the relaxation time spectra $H(\tau)$ calculated from the dynamic moduli and the MWD.

Table V. Viscosity Ratio, Droplet Shape Relaxation Time, and Interfacial Tension of the Model Compounds According to the Models of Palierne and Gramespacher–Meissner

	Viscosity ratio η (dispersed phase)/η (matrix)	Droplet form relaxation time τ_1 (s)	Interfacial tension (α) according to Palierne (mN m^{-1})	Interfacial tension (α) according to Gramespacher–Meissner (mN m^{-1})
PPEO20	1.8	13.2	0.35	0.94
PPLD20	1.5	20.3	0.01	0.80
PPHD20	1.1	-	-	-
RPEO20	1.4	31.1	0.26	0.57
RPLD20	1.3	47.9	0.01	0.38
RPHD20	0.9	-	-	-

and rheological analyses, interactions between inclusion and matrix are most likely in the blends based on the random copolymer.

The determination of the interfacial tension for the blends modified with the HDPE resulted in some problems as the dynamic moduli of these blends do not show their typically three-domain behavior[16] with the terminal zone of the emulsion where G' falls proportional to ω^2 and G'' to ω at low frequencies. Even at frequencies smaller than 0.01 rad s^{-1}, the G' curves tend to increase. This shape of the curve is due to the used modifier, which also does not reach the linear range in the measured frequency region. As no satisfying correlation between measured and calculated curves could be found for these systems, no values for interfacial tension were obtained.

A decrease in interfacial tension was found for blends based on the same polymer from the EOC plastomer to the LLDPE. A possible reason is the presence of long comonomer units (C8) in the plastomer, which are also decisive for the reduced crystallizability. Furthermore, it is the only modifier having a density below that of the base polymer. The difference in α between plastomer and LLDPE was not expected to be so high and cannot be fully explained at present.

If the base polymer is changed from the PP to the EP random copolymer, the interfacial tension decreases slightly, which means that the compatibility of the modifiers with the copolymer is better than with the PP homopolymer. This most likely results from the higher similarity of modifier and matrix as a result of the ethylene units and the polyethylene blocks present in the EP copolymer chain.

Some of the deviations might result from the fact that the curves could not be completely fitted. The fit could not be improved by using higher values of α/r as the sensitivity of the calculated curve to this factor was not pronounced. These analyses demonstrate that the applicability of Palierne's emulsion model for blends with semicrystalline modifiers is limited.

Gramespacher–Meissner Analysis

If the moduli of polymer blends are assumed to consist of two contributions that are caused by the rheological properties of the components as well as by the interfacial tension, one obtains the following relationship for loss and storage moduli of polymer blends:

$$G*(\omega) = \Phi G*(\omega)_i + (1-\Phi)G*(\omega)_m + G*(\omega)_i. \qquad (13)$$

The parameters have the same meaning as in eqs. (11) and (12). Gramespacher and Meissner[17] developed the following description for the storage and the loss moduli in which the interfacial contribution is expressed as a modulus:

$$G'(\omega)_b = \Phi G'(\omega)_i + (1-\Phi)G'(\omega)_m + \frac{\eta}{\tau_1}\left(1-\frac{\tau_2}{\tau_1}\right)\frac{\omega^2\tau_1^2}{1+\omega^2\tau_1^2}, \qquad (14)$$

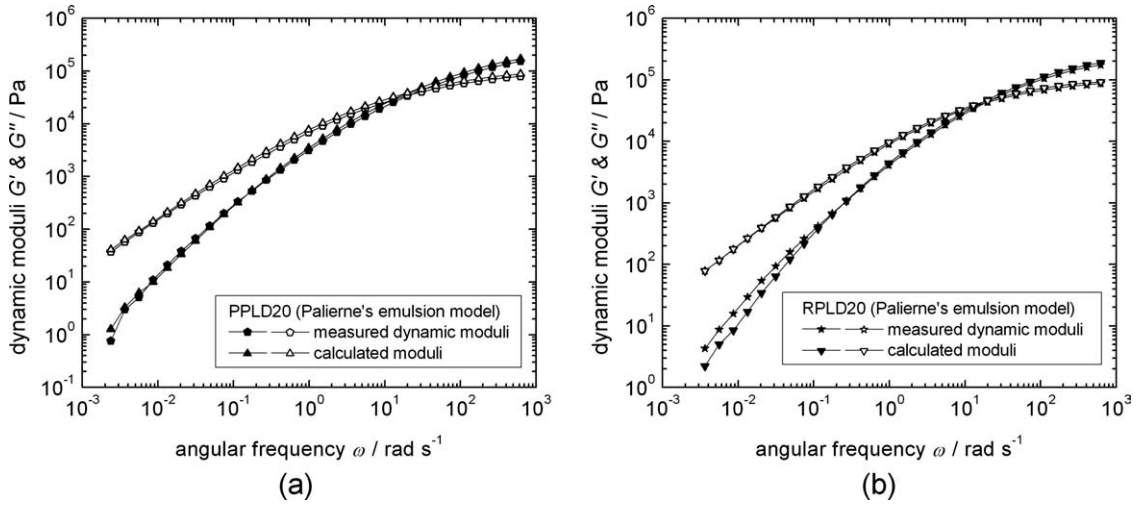

Figure 10. Dynamic moduli measured and calculated according to Palierne's emulsion model (T = 200°C, N_2 atmosphere): (a) PPLD20 and (b) RPLD20.

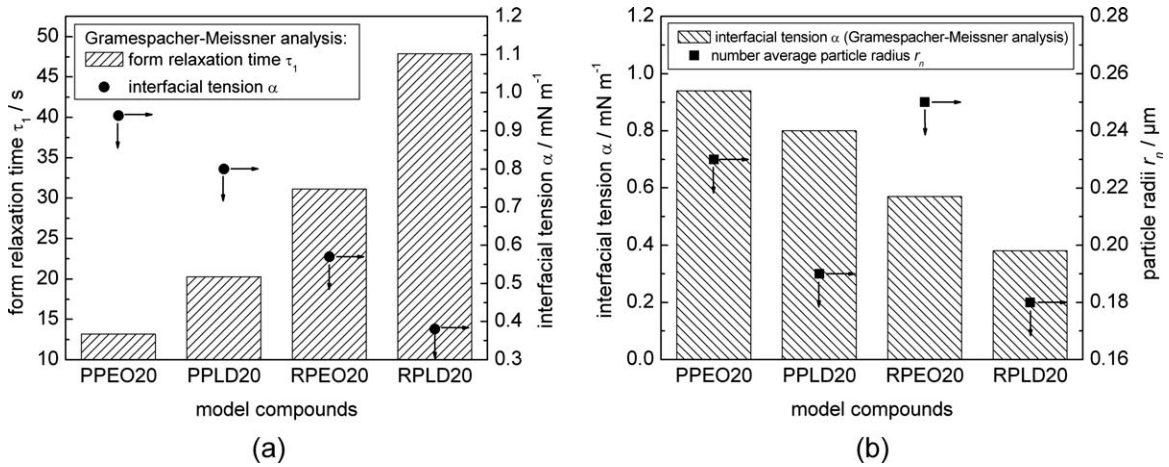

Figure 11. Relationships between form relaxation time, interfacial tension, and particle size: (a) form relaxation time compared with interfacial tension and (b) interfacial tension compared with particle radii.

$$G''(\omega)_b = \Phi G''(\omega)_i + (1-\Phi)G''(\omega)_m + \frac{\eta}{\tau_1}\left(1-\frac{\tau_2}{\tau_1}\right)\frac{\omega\,\tau_1}{1+\omega^2\tau_1^2}. \tag{15}$$

The parameters for this modulus are defined as follows:

$$\eta = \eta_{0,m}\left[1+\Phi\frac{(5k+2)}{2(k+1)}+\Phi^2\frac{5(5k+2)^2}{8(k+1)^2}\right], \tag{16}$$

$$\tau_1 = \tau_0\left[1+\Phi\frac{5(19k+16)}{4(k+1)(2k+3)}\right], \tag{17}$$

$$\tau_2 = \tau_0\left[1+\Phi\frac{3(19k+16)}{4(k+1)(2k+3)}\right], \tag{18}$$

$$\tau_0 = \frac{\eta_{0,m}R}{\alpha}\cdot\frac{(19k+16)(2k+3)}{40(k+1)}, \tag{19}$$

$$k = \frac{\eta_{0,d}}{\eta_{0,m}}. \tag{20}$$

The influence of the interfacial tension on the viscoelastic properties is only present in the low frequency range. At these frequencies, the storage modulus is much smaller than the loss modulus, which means that the viscoelastic behavior is predominantly governed by the zero-shear viscosities. This fact is the reason why for all above shown equations, the zero-shear viscosities of dispersed phase and matrix can be used. The shape relaxation time τ_1, which is proportional to the interfacial tension α, can be determined directly from the weighted relaxation time spectra as it is visible as an additional peak at a relaxation time equal to τ_1. Consequently, the relaxation spectrum of an immiscible polymer blend is a combination of the relaxation spectra of the pure components and an additional peak around τ_1 due to the interfacial interaction. In the literature, it is reported that the applicability of this model might also be given in cases where Palierne's model does not deliver promising results.[43] The values of α obtained in this way are listed in Table IV.

These values differ strongly from the ones found with Palierne's emulsion model; however, the values are in a range comparable with those reported in the literature.[41,44] For a comparison of the blends based on the PP homopolymer and the EP random copolymer, the same trends as determined with the aid of

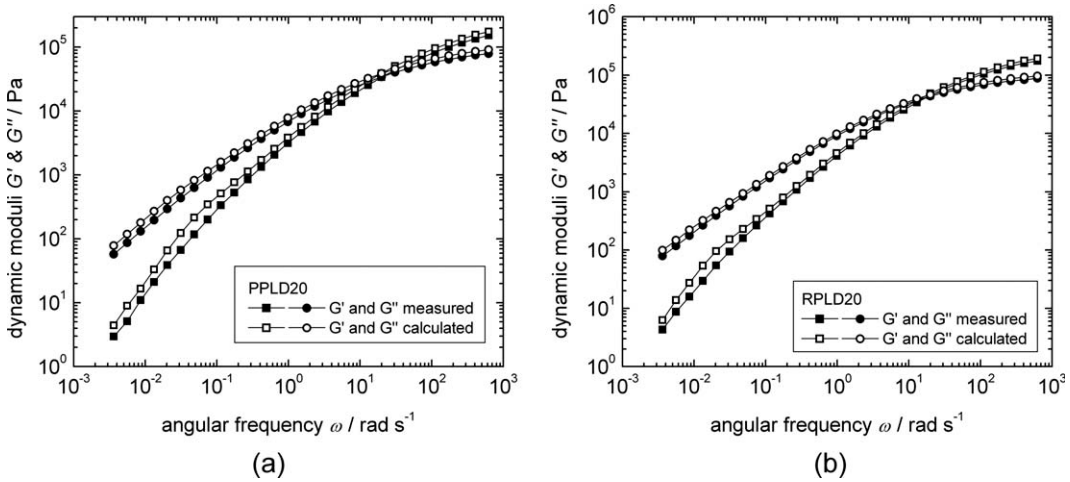

Figure 12. Dynamic moduli measured and calculated with Gramespacher–Meissner analysis for (a) PPLD20 and (b) RPLD20.

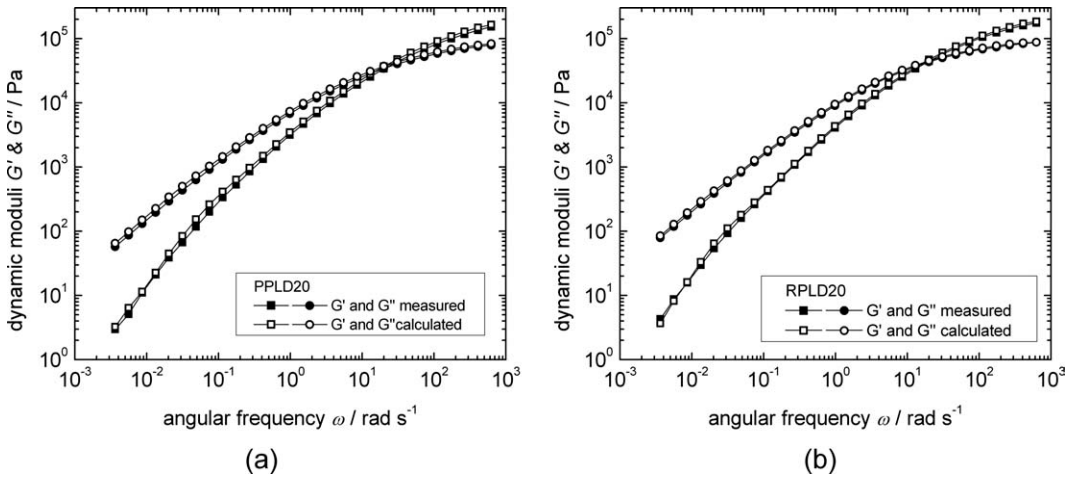

Figure 13. Dynamic moduli measured and calculated with Gramespacher–Meissner analysis. The calculations were performed for blends containing only 9% of immiscible dispersed phase, that is, by assuming 11% miscibility: (a) PPLD20 and (b) RPLD20.

Palierne's emulsion model are found. The relationship between droplet shape relaxation time, interfacial tension, and particle size is shown for four model compounds in Figure 11. Blends having long droplet shape relaxation times show low interfacial tensions. The interfacial tension is directly proportional to the particle size, but it is not the only influencing factor on blend morphology (see "Blend Morphology" section). This is the reason why EPPL20 has bigger particles than PPPL20 although its interfacial tension is smaller.

By substituting these values in eqs. (14) and (15), the dynamic moduli of the blends can be calculated from those of the components. However, a comparison between measured and calculated curves shows that the correspondence is not higher than that by applying Palierne's emulsion model. For PPLD20 and EPLD20, the calculated moduli are shifted to higher values and show a more pronounced increase of G' at low frequencies (Figure 12).

The correspondence can be improved by accounting for the partial miscibility in the molten state indicated by rheological investigations and morphology analyses of the PPLD and RPLD blends. The results of these calculations showed that an almost perfect fit can be achieved if the amount of dispersed phase in the calculations was set to 9% instead of 20% (see Figure 13). The result underlines the assumption that the used PP and the EP random copolymer are not totally immiscible with the LLDPE.

CONCLUSIONS AND OUTLOOK

As expected, all mixtures show a clear multiphase structure with the base material as matrix and the modifier as inclusions, where the inclusions consist of amorphous parts and crystalline PE if LLDPE or HDPE is used as modifier. The observation of PE lamellae in the PP matrix was not expected and is an indication for partial miscibility of the components in the melt. This phenomenon is clearly further supported by the rheological investigations.

The investigated model blend series clearly shows that the type of modifier and matrix phase essentially influences the compatibility and degree of interaction between matrix and dispersed phase in the melt. The interfacial tension calculated via Gramespacher–Meissner analysis from the continuous relaxation time spectra revealed a clear diminishing tendency, with changing the matrix phase from a homopolymer to a random copolymer. This reflects an increasing compatibility between the two phases with the introduction of ethylene in the matrix. A substitution of the EOC by an LLDPE further decreases the interfacial tension. The viscosity of the blends corresponded to the one calculated via the logarithmic mixing rule up to 10 wt % PE, confirming miscibility of LLDPE with the PP homopolymer and the random copolymer. Phase separation takes place on solidification as PP and PE show different crystallization behavior, resulting in PE lamellae appearing isolated in the matrix or across the interface between matrix and modifier.

This study also demonstrates that the applicability of the Palierne's emulsion model for blends with semicrystalline modifiers is limited, as no total correlation of calculated and measured curves for the copolymer-based blends was achieved. The applicability of the Gramespacher–Meissner analysis is clearly better for the investigated model compounds, and the curves calculated according to this model fit perfectly to the measured ones if one takes a partial miscibility of matrix and dispersed phase into account. Furthermore, the values for the interfacial tension obtained by Gramespacher–Meissner analysis were in the range already reported in the literature.[41,44]

The morphology of polymer blends is strongly affected by both the viscosity ratio between matrix and dispersed phase and by the compatibility. In view of similar viscosity ratios in the model compounds, the decrease in particles size of the inclusions when changing from the EOC plastomer to the LLDPE can be well explained with the reduced interfacial tension. The improved compatibility when changing the matrix polymer from the homopolymer to the random copolymer allows developing multiphase materials with finer phase structure, which

will also result in improved mechanical and optical performance. Details of the possibilities in terms of fracture behavior and transparency will be reported in the second part of this study.

REFERENCES

1. Pasquini, N., Ed. Polypropylene Handbook, 2nd ed.; Hanser: Munich, **2005.**
2. Walter, P.; Mäder, D.; Reichert, P.; Mülhaupt, R. *J. Macromol. Sci. Part A* **1999,** *36*, 1613.
3. Martuscelli, E. In Polypropylene Structure, Blends and Composites; Karger-Kocsis, J., Ed.; Chapman and Hall: London, **1995;** Vol. *2*: Copolymers and Blends, p 95.
4. Stricker, F.; Thomann, Y.; Mülhaupt, R. *J. Appl. Polym. Sci.* **1998,** *68*, 1891.
5. Schwager, H. In PP Reactor Blends, Paper Presented at the Polypropylene 1992 World Congress, Zürich/CH, II-4.1, October 27–28, **1992.**
6. Yu, T. C. *Polym. Eng. Sci.* **2001,** *41*, 656.
7. Gahleitner, M.; Hauer, A.; Bernreitner, K.; Ingolic, E. *Intern. Polym. Proc.* **2002,** *17*, 318.
8. Kontopoulou, M.; Wang, W.; Gopakumar, T. G.; Cheung, C. *Polymer* **2002,** *43*, 3785.
9. Grein, C.; Bernreitner, K.; Hauer, A.; Gahleitner, M.; Neißl, W. *J. Appl. Polym. Sci.* **2003,** *87*, 1702.
10. Grein, C.; Gahleitner, M.; Knogler, B.; Nestelberger, S. *Rheol. Acta* **2007,** *46*, 1083.
11. Tortorella, N.; Beatty, C. L. *Polym. Eng. Sci.* **2008,** *48*, 2098.
12. Soares, J. B. P.; Hamielec, A. E. *Polymer* **1995,** *36*, 1639.
13. Aust, N.; Gahleitner, M.; Reichelt, K.; Raninger, B. *Polym. Test.* **2006,** *25*, 896.
14. Kissin, Y. V.; Fruitwala, H. A. *J. Appl. Polym. Sci.* **2007,** *106*, 3872.
15. Fischlschweiger, M.; Aust, N.; Oberaigner, E. R.; Kock, C. *Macromol. Chem. Phys.* **2009,** *210*, 383.
16. Graebling, D.; Muller, R.; Palierne, J. F. *Macromolecules* **1993,** *26*, 320.
17. Gramespacher, H.; Meissner, J. J. *Rheol.* **1992,** *36*, 1127.
18. Pölt, P.; Ingolic, E.; Gahleitner, M.; Bernreitner, K.; Geymayer, W. *J. Appl. Polym. Sci.* **2000,** *78*, 1152.
19. Svoboda, P.; Svobodova, D.; Slobodian, P.; Ougizawa, T.; Inoue, T. *Eur. Polym. J.* **2009,** *45*, 1485.
20. Lee, H.-Y.; Kim, D. H.; Son, Y. *J. Appl. Polym. Sci.* **2007,** *103*, 1133.
21. Svoboda, P.; Theravalappil, R.; Svobodova, D.; Mokrejs, P.; Kolomaznik, K.; Mori, K.; Ougizawa, T.; Inoue, T. *Polym. Test.* **2010,** *29*, 742.
22. Montezinos, D.; Wells, B. G.; Burns, J. L. *J. Polym. Sci. Polym. Lett. Ed.* **1985,** *23*, 421.
23. Abramhoff, M. D.; Magelahaes, P. J.; Ram, S. J. *Biophotonics Int.* **2004,** *11*, 36.
24. Mathot, V. B. F. In Thermal Characterization of States of Matter; Mathot, V. B. F., Ed.; Hanser Publishers: Munich, **1994;** p 103.
25. Winter, H. H. *Rheol. Acta* **2009,** *48*, 241.
26. Gahleitner, M. *Prog. Polym. Sci.* **2001,** *26*, 895.
27. Wesslau, H. *Die Makromol. Chem.* **1956,** *20*, 111.
28. Van den Eyn, S.; Mathot, V. B. F.; Koch, M. H. J.; Reynaers, H. *Polymer* **2000,** *41*, 4889.
29. Kim, M. H.; Alamo, R. G.; Lin, J. S. *Polym. Eng. Sci.* **1999,** *39*, 2117.
30. Starke, J. U.; Michler, G. H.; Grellmann, W.; Seidler, S.; Gahleitner, M.; Fiebig, J.; Nezbedova, E. *Polymer* **1998,** *39*, 75.
31. Tan, H.; Li, L.; Chen, Z.; Song, Y.; Zheng, Q. *Polymer* **2005,** *46*, 3522.
32. Benham, E.; McDaniel, M. Ethylene Polymers, HDPE; Encyclopedia of Polymer Science and Technology; Wiley: New York, **2010**.
33. Li, J.; Shanks, R. A.; Long, Y. *J. Appl. Polym. Sci.* **2001,** *82*, 628.
34. Shanks, R. A.; Li, J.; Yu, L. *Polymer* **2000,** *41*, 2133.
35. Li, J.; Shanks, R. A.; Long, Y. *Polymer* **2001,** *42*, 1941.
36. Honerkamp, J.; Weese, J. *Macromolecules* **1989,** *22*, 4327.
37. Honerkamp, J.; Weese, J. *Rheol. Acta* **1993,** *32*, 65.
38. Schausberger, A. *Rheol. Acta* **1986,** *25*, 596.
39. Schausberger, A. *Rheol. Acta* **1991,** *30*, 197.
40. Palierne, J. F. *Rheol. Acta* **1991,** *29*, 204.
41. Souza, A. M. C.; Demarquette, N. R. *Polymer* **2002,** *43*, 1313.
42. Vincze-Minya, K. A.; Schausberger, A. *Chem. Mon.* **2006,** *137*, 911.
43. Calvao, P.; Yee, M.; Demarquette, N. R. *Polymer* **2005,** *46*, 2610.
44. Souza, A. M. C.; Demarquette, N. R. *Polymer* **2002,** *43*, 3959.